Radiology: Cardiothoracic Imaging

ORIGINAL RESEARCH

Serial Quantitative Chest CT Assessment of COVID-19: A Deep Learning Approach

Lu Huang, MD, PhD • Rui Han, MD • Tao Ai, MD, PhD • Pengxin Yu, MS • Han Kang, MS • Qian Tao, PhD • Liming Xia, MD, PhD

From the Department of Radiology, Tongji Hospital, Tongji Medical College, Huazhong University of Science and Technology, Jiefang Avenue 1095, 430030 Wuhan, China (L.H., T.A., L.X.); Department of Radiology, Wuhan No. 1 Hospital, Wuhan, China (R.H.); Institute of Advanced Research, Infervison, Beijing, China (P.Y., H.K.); and Division of Imaging Processing, Department of Radiology, Leiden University Medical Center, Leiden, the Netherlands (Q.T.). Received February 20, 2020; revision requested March 11; final revision received March 17; accepted March 20. **Address correspondence to** L.X. (e-mail: *lmxia@tjh.tjmu.edu.cn*).

Funding support was provided for this study by the Wuhan Science and Technology Program (grant no. 2018060401011326), Hubei Provincial Novel Pneumonia Emergency Science and Technology Project (grant no. 2020FCA021), and Huazhong University of Science and Technology Novel Coronavirus Pneumonia Emergency Science and Technology Project (grant no. 2020kfyXGYJ014).

Conflicts of interest are listed at the end of this article.

Radiology: Cardiothoracic Imaging 2020; 2(2):e200075 • https://doi.org/10.1148/ryct.2020200075 • Content codes: AI CH

Purpose: To quantitatively evaluate lung burden changes in patients with coronavirus disease 2019 (COVID-19) by using serial CT scan by an automated deep learning method.

Materials and Methods: Patients with COVID-19, who underwent chest CT between January 1 and February 3, 2020, were retrospectively evaluated. The patients were divided into mild, moderate, severe, and critical types, according to their baseline clinical, laboratory, and CT findings. CT lung opacification percentages of the whole lung and five lobes were automatically quantified by a commercial deep learning software and compared with those at follow-up CT scans. Longitudinal changes of the CT quantitative parameter were also compared among the four clinical types.

Results: A total of 126 patients with COVID-19 (mean age, 52 years ± 15 [standard deviation]; 53.2% males) were evaluated, including six mild, 94 moderate, 20 severe, and six critical cases. CT-derived opacification percentage was significantly different among clinical groups at baseline, gradually progressing from mild to critical type (all $P < .01$). Overall, the whole-lung opacification percentage significantly increased from baseline CT to first follow-up CT (median [interquartile range]: 3.6% [0.5%, 12.1%] vs 8.7% [2.7%, 21.2%]; $P < .01$). No significant progression of the opacification percentages was noted from the first follow-up to second follow-up CT (8.7% [2.7%, 21.2%] vs 6.0% [1.9%, 24.3%]; $P = .655$).

Conclusion: The quantification of lung opacification in COVID-19 measured at chest CT by using a commercially available deep learning–based tool was significantly different among groups with different clinical severity. This approach could potentially eliminate the subjectivity in the initial assessment and follow-up of pulmonary findings in COVID-19.

Supplemental material is available for this article.

Severe acute respiratory syndrome coronavirus 2 (SARS-CoV-2) is a novel coronavirus initially identified in Wuhan, China, which causes a respiratory pandemic disease named coronavirus disease 2019 (COVID-19) (1–5). Chest CT has played a pivotal diagnostic role in the assessment of patients with COVID-19 in China (6).

Recent studies reported that the possible pathologic mechanism in COVID-19 is diffuse alveolar damage and inflammatory exudation, which is similar to histologic findings seen in severe acute respiratory syndrome coronavirus pneumonia (1,7). The pathologic evolution during the course of infection in COVID-19 has not been clarified, and the disparity of such changes in patients with different clinical severities is largely unknown. Chest CT, especially thin-section CT, can detect small areas of ground-glass opacity (8) and, therefore, is a promising imaging tool for monitoring the disease, if radiation dose is balanced to comply with ALARA (as low as reasonably achievable) principles. It is common practice for radiologists to evaluate pneumonia severity qualitatively or semiquantitatively by visual scoring (9). Visual evaluation of changes between two CT scans is subjective, and its validity may depend on the radiologists' experience. Quantitative analysis of the CT scans using an artificial intelligence tool, in particular deep learning, could provide an automatic and objective estimation of the disease burden, facilitating and expediting imaging interpretation during the COVID-19 pandemic (10).

This study aimed to assess a quantitative CT image parameter, defined as the percentage of lung opacification (QCT-PLO), which is calculated automatically using a deep learning tool. We evaluated QCT-PLO in patients with COVID-19 at baseline and on follow-up scans, focusing on cross-sectional and longitudinal differences in patients with different degrees of clinical severity.

Materials and Methods

The local ethical review board approved this retrospective study and waived the requirement to obtain individual informed consent.

Abbreviations

COVID-19 = coronavirus disease 2019, hs-CRP = high-sensitivity C-reactive protein, QCT-PLO = quantitative CT percentage of lung opacification, SARS-Cov-2 = severe acute respiratory syndrome coronavirus 2

Summary

The quantification of lung opacification measured at chest CT using a commercially available deep-learning-based tool may be used to monitor the disease progression and understand the temporal evolution of COVID-19.

Key Points

- The quantitative CT parameter calculated by the deep learning method showed significant differences at baseline among four clinical types (all $P < .01$).
- Lung opacification percentage may be used to monitor disease progression and help understand the course of COVID-19.

Study Population

Patients with COVID-19, who underwent chest CT in our department from January 1 to February 3, 2020, were enrolled in this retrospective study. Inclusion criteria were as follows: *(a)* positive SARS-Cov-2 nucleic acid in double swab tests (within an interval of 2 days, real-time reverse-transcription polymerase chain reaction), *(b)* with at least two chest CT scans in our hospital, and *(c)* without confirmation of another viral infection. Exclusion criteria were as follows: *(a)* patients who underwent initial chest CT in other hospitals, *(b)* CT images with respiratory artifacts that could not meet the image analysis requirement, or *(c)* inadequate deep learning segmentation by the segmentation algorithm based on the radiologist's review, as explained in detail later. Figure 1 shows the patient enrollment flowchart.

At baseline, all patients were classified into four clinical types: mild, moderate, severe, and critical, according to the Diagnosis and Treatment Protocol of Novel Coronavirus (trial version 5) (6) from the National Health Commission of the People's Republic of China. The classification criteria of clinical types are described in Appendix E1 (supplement).

CT Scanning

Non–contrast-enhanced chest CT examinations were performed using three CT scanners (United Imaging uCT, United Imaging Healthcare, Shanghai, China; GE Optima 660, GE Healthcare, Chicago, Ill; Siemens SOMATOM Definition AS+, Siemens Healthineers, Erlangen, Germany). The patients were scanned in the supine position during inspiratory breath hold. The scanning range was from the apex to the base of the lungs. Scanning parameters were as follows: tube voltage 80–120 kV, tube current 50–350 mAs, pitch 0.99–1.22 mm, matrix 512 × 512, slice thickness 10 mm, and field of view 350 × 350 mm. Reconstruction was performed with a slice thickness of 0.625–1.250 mm, a lung window with a width of 1200 HU and a level of −600 HU, and a mediastinal window with a width of 350 HU and a level of 40 HU.

CT Image Analysis

Quantitative analysis of lung opacification was performed using a deep learning algorithm. This algorithm consists of three modules: *(a)* lung and lobes segmentation module, *(b)* lung opacity segmentation module, and *(c)* quantitative analysis module. The algorithms used in *(a)* and *(b)* were based on a deep learning framework to learn the complex relationship between diverse features extracted from chest CT scans and regions of interest (lungs, lobes, and opacities). The deep learning algorithm in module *(b)* employed a well-established, fully convolutional neural network architecture (11) trained on annotated datasets of COVID-19. We describe the deep learning algorithms in detail in Appendix E2 (supplement). On the basis of the segmentation results of lungs and lesions, the workstation provided a quantitative measure of lung opacification percentage (Fig 2).

Accurate segmentation of the lung opacities was the basis for quantitative analysis. Hence, all segmentation results derived from this deep learning algorithm were visually evaluated by two radiologists (L.H., with 7 years of experience in cardiopulmonary imaging and R.H., with 8 years of experience in pulmonary imaging), who viewed the segmentation independently. Both radiologists were blinded to the patient's clinical status. The scoring procedure was as follows: both radiologists reviewed the segmentation results displayed as regions of interest overlaid on the CT images slice-by-slice. The readers did not adjust the automatic segmentation. The readers used scoring criteria based on the adequacy of the segmentation task versus actual lung opacification. Specifically, the degree of matching was quantified using a Likert score from 0 to 5. The scoring criteria is described in detail in Appendix E3 (supplement). To reduce the subjectivity of the radiologist's evaluation, the final score was the average of two scores for each scan. A final score ≥3 was considered as sufficient to meet the quantitative analysis requirement.

Statistical Analysis

Statistical analysis was performed using SPSS software (version 23.0, IBM statistics, Armonk, NY). Categorical variables were expressed as counts (percentage), and continuous variables as mean ± standard deviation or median (interquartile range). Normality of distribution was tested using the Kolmogorov-Smirnov test. The difference between two paired groups was assessed by paired *t* test or the Wilcoxon test. Moreover, comparisons among different clinical types were performed using the analysis of variance or Kruskal-Wallis test. Comparison between any of the two clinical types was performed by *t* test or Mann-Whitney *U* test for continuous variables and χ^2 test for categorical variables. Low-frequency variables were compared with the Fisher exact test. Two-sided $P < .05$ was considered statistically significant.

Results

Clinical Characteristics

In this study, 148 patients with COVID-19 were initially enrolled, with nine (6.1%) patients excluded because of respira-

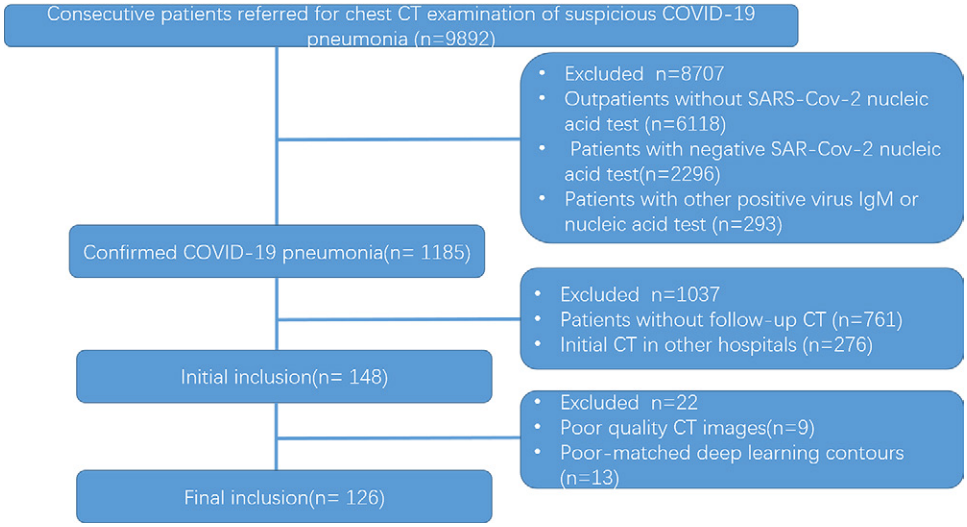

Figure 1: Flowchart shows the patient selection process. IgM = immunoglobulin M.

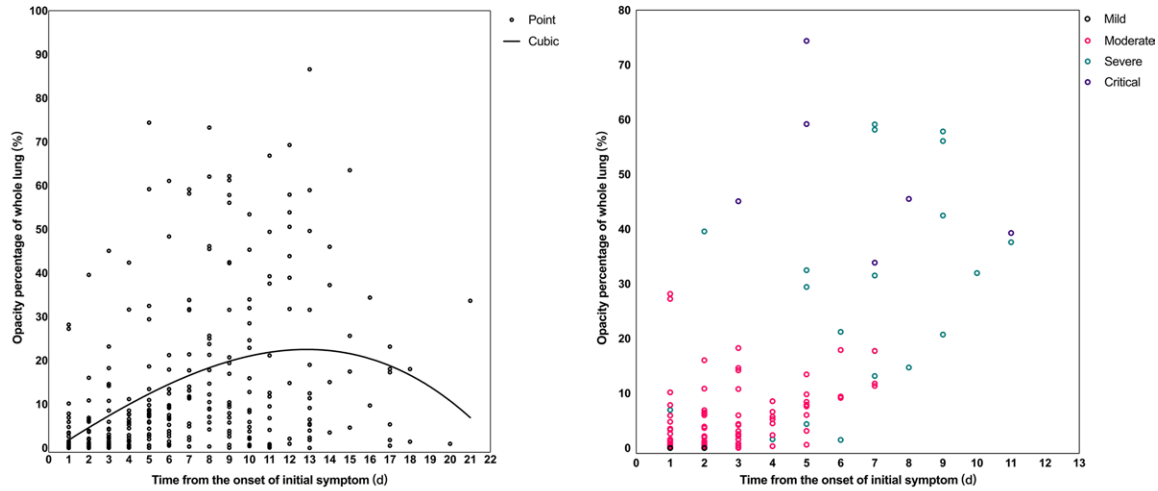

a. b.

Figure 2: Scatterplots with the distribution of lung opacification percentage according to days since initial symptoms. **(a)** The dynamic change in lung opacification percentage of whole lung (curve fitting equation: $y = 2.956 \times x^3 - 0.03065 \times x^2 - 0.004374 \times x - 1.106$, in which x is time from the onset of initial symptoms, y is lung opacification percentage of whole lung; $R^2 = 0.161$, $P < .001$). **(b)** The distribution of percentage of lung opacification at quantitative CT in different clinical types according to days since initial symptoms at baseline CT.

tory motion artifacts and 13 (8.7%) excluded because of insufficient segmentation quality, as determined from the scores provided by the two radiologists (ie, mean score < 3). Finally, 126 patients (mean age, 52 years ± 15; age range, 14–86 years; 53.2% males) with COVID-19 were included. Baseline characteristics of patients with COVID-19 are summarized in Table 1. All patients were classified into four clinical types, including six mild cases (4.8%), 94 moderate cases (74.6%), 20 severe cases (15.8%), and six critical cases (4.8%). The median of interval between baseline and first follow-up was 4 days (interquartile range, 3–6 days), and the median of interval between the first and second follow-ups was 5 days (interquartile range, 3–7 days).

Age and sex had no significant difference among the different clinical types of COVID-19 ($P > .05$). The duration between onset symptoms and initial CT scanning of mild and moderate type patients was shorter than that of severe and critical type patients (all $P < .01$). In 117 of 126 (92.9%) patients, fever was the initial symptom, while dyspnea was only observed in severe and critical type patients. Of the laboratory findings, white blood cell count, lymphocyte count, high-sensitivity C-reactive protein (hs-CRP), and pulse oxygen saturation showed significant differences among the four clinical types of patients (all $P < .05$). Compared with critical type patients, white blood cell count and hs-CRP were significantly lower in the moderate type cases (both $P < .001$), but the lymphocyte count was higher ($P = .004$).

Quantitative CT Parameters at Baseline and at First and Second Follow-up CT Scans

All 126 patients underwent two CT scans as per inclusion criteria, and 48 of 126 (38.1%) patients underwent three CT

Table 1: Baseline Characteristics of Patients with COVID-19, according to Clinical Severity

Variable	COVID-19 (n = 126)	Mild Type (n = 6)	Moderate Type (n = 94)	Severe Type (n = 20)	Critical Type (n = 6)	P Value*
Age (year)†	52 ± 15	47 ± 15	51 ± 16	56 ± 13	66 ± 8	.074
Sex (male)	67 (53.2)	3 (50.0)	49 (52.1)	11 (55.0)	4 (66.7)	.946
Duration between onset symptoms and the initial CT scanning†	2.5 (1, 5)	1 (1, 1)	2 (1, 3)	6.5 (5, 7.3)	6 (5, 7.8)	< .001
Comorbidity						
Hypertension	10 (7.9)	1 (16.7)	4 (5.3)	2 (10.0)	3 (50)	.018
Diabetes	7 (5.6)	0	3 (3.2)	2 (10.0)	2 (33.3)	.036
COPD	2 (1.6)	1 (16.7)	0	0	1 (16.7)	.008
CAD	7 (5.6)	0	4 (4.3)	1 (5.0)	2 (33.3)	.085
Symptoms						
Fever	117 (92.9)	6 (100)	85 (90.4)	20 (100)	6 (100)	.598
Normal	9 (7.1)	0	9 (9.6)	0	0	< .001
37.3°C –38.0°C	8 (6.3)	1 (16.7)	7 (8.2)	0	0	.344
38.1°C –39.0°C	94 (74.6)	4 (66.7)	78 (91.8)	11 (55.0)	1 (16.7)	< .001
≥39.1°C	15 (11.9)	1 (16.7)	0	9 (45.0)	5 (83.3)	< .001
Cough	35 (27.8)	3 (50)	22 (23.4)	9 (45.0)	1 (16.7)	.202
Fatigue	19 (15.1)	0	14 (14.9)	5 (25.0)	0	.416
Dyspnea	14 (11.1)	0	0	8 (40.0)	6 (100)	< .001
Chest distress	9 (7.1)	0	7 (7.4)	2 (10.0)	0	.865
Headache	5 (4.0)	0	3 (3.2)	2 (10.0)	0	.526
Diarrhea	4 (3.2)	0	4 (4.3)	0	0	1.000
Sore throat	2 (1.6)	0	1 (1.2)	1 (5.0)	0	.445
Laboratory findings						
WBC count ($\times 10^9$/L)†	4.8 (3.8, 6.1)	3.2 (3.1, 5.7)	4.6 (3.8, 5.8)	6.3 (5.0, 11.7)	8.1 (6.7, 9.3)	.014
Lymphocyte count ($\times 10^9$/L)†	0.9 (0.7, 1.3)	0.7 (0.7, 1.0)	1.1 (0.9, 1.3)	0.8 (0.7, 0.9)	0.6 (0.5, 0.7)	.016
hs-CRP (mg/L)†	18.9 (10.2, 45.7)	11.7 (10.85, 14.65)	16.1 (10.1, 25.7)	97.4 (34.6, 122.5)	123.9 (114.6, 136.3)	< .001
SpO_2 < 90	26 (20.6)	0	0	20 (100)	6 (100)	< .001

Note.—Unless otherwise specified, data are numbers, with percentages in parentheses. CAD = coronary artery disease, COPD = chronic obstructive pulmonary disease, hs-CRP = high-sensitivity C-reactive protein, SpO_2 = pulse oxygen saturation, WBC = white blood cell.

* P value is for four clinical types. $P < .05$ is considered to indicate statistical significance.

† Data are means ± standard deviations with normal distribution or median (interquartile range) with nonnormal distribution.

scans. Of 300 CT scans, 236 (78.6%) had a segmentation quality score in the range of 3–4, and 64 (21.4%) CT scans were in the range of 4–5.

The distribution of lung opacification percentage of all patients according to days since the onset of symptoms is shown in Figure 2a, and the peak lung opacification percentage of whole lung occurred on day 13. Overall, the whole-lung QCT-PLO significantly increased from baseline CT to first follow-up CT (median [interquartile range]: 3.6% [0.5%, 12.1%] vs 8.7% [2.7%, 21.2%]; $P < .01$). No significant progression of whole-lung QCT-PLO was noted from the first follow-up to the second follow-up CT (8.7% [2.7%, 21.2%] vs 6.0% [1.9%, 24.3%]; P = .655). Percentage changes in the CT-derived opacification parameters at the first and second follow-ups are shown in Table 2.

Quantitative CT Opacification Parameters in Different Clinical Types of Patients with COVID-19

Differences in whole-lung QCT-PLO according to clinical severity subtype and days since onset of symptoms at baseline CT are shown in Figure 2b.

Significant differences in QCT-PLO were found among the four different clinical types at baseline and at the first follow-up (all $P < .05$; Table 3). All of the six mild type patients with COVID-19 had negative results at baseline CT and were found

Table 2: Percentage Changes in QCT-PLO at First and Second Follow-up

Percentage Change	First Follow-up	Second Follow-up
Total opacification percentage of whole lung	69.3 (−14.5, 605.8)	3.0 (−59.1, 223.0)
Opacification percentage of right upper lobe	0 (−12.0, 170.9)	0 (−43.2, 93.4)
Opacification percentage of right middle lobe	0 (−30.9, 47.9)	0 (−86.3, 54.0)
Opacification percentage of right lower lobe	14.1 (−14.5, 431.9)	0 (−68.0, 155.8)
Opacification percentage of left upper lobe	0 (−10.5, 163.4)	0 (−52.7, 135.1)
Opacification percentage of left lower lobe	0.7 (9.1, 370.6)	0 (−74.9, 453.5)

Note.—Unless otherwise specified, data are median (interquartile range). QCT-PLO = quantitative CT-percentage of lung opacification.

Table 3: QCT-PLO according to Clinical Severity in COVID-19, Baseline CT

Parameter	Mild Type (n = 6)	Moderate Type (n = 94)	Severer Type (n = 20)	Critical Type (n = 6)	P Value*
Total opacification percentage of whole lung	0	2.2 (0.4, 7.1)	28.9 ± 19.2†	49.6 ± 14.8†	< .001
Opacification percentage of right upper lobe	0	0.4 (0, 2.7)	28.1 ± 21.0†	56.2 ± 21.9†	< .001
Opacification percentage of right middle lobe	0	0.2 (0, 1.8)	24.5 ± 20.4†	42.3 ± 25.9†	< .001
Opacification percentage of right lower lobe	0	2.9 (0.2, 13.6)	43.3 ± 30.7†	61.1 ± 17.7†	< .001
Opacification percentage of left upper lobe	0	0.3 (0, 3.0)	12.3 (4.4, 22.6)†	44.8 ± 24.8†‡	< .001
Opacification percentage of left lower lobe	0	1.3 (0, 7.0)	33.3 ± 21.8†	42.8 ± 34.0†	< .001

Note.—Unless otherwise specified, data are means ± standard deviation with normal distribution or median (interquartile range) with nonnormal distribution. QCT-PLO = quantitative CT-percentage of lung opacification.
* P value is for four clinical types. $P < .05$ is considered to indicate statistical significance.
† P value < .05 divided by 6 compared with moderate type.
‡ P value < .05 divided by 6 compared with severe type.

to have positive results at the first follow-up CT scan (Fig 3). QCT-PLO of right and left lower lobes were elevated at the second follow-up CT scan (both $P < .05$; Table E1 [supplement]). Compared with baseline CT scan, whole-lung and per-lobe QCT-PLO increased significantly in moderate type patients (all $P < .05$; Appendix E3 [supplement]) (Fig 4), while no remarkable difference was found between the first and second follow-up scans (all $P > .05$; Table E2 [supplement]). In severe and critical type patients, the whole-lung and per-lobe QCT-PLO showed no significant differences between baseline and first or second follow-up CT (Figs 5 and 6, respectively).

Discussion

In this study, we evaluated the longitudinal changes of pneumonia severity in different clinical types of COVID-19 at baseline and follow-up imaging by using a quantitative image parameter (QCT-PLO), which was automatically generated by a deep learning tool from chest CT scans. Our major findings were as follows: *(a)* this quantitative parameter based on deep learning could identify differences in the lung opacity burden on CT from patients with COVID-19 of different clinical severities, and *(b)* overall, the whole-lung and per-lobe QCT-PLO at the first follow-up CT increased in comparison with those at baseline scans (median interval, 4 days), while no remarkable progress was found at the second follow-up (median interval, 5 days).

Patients with mild and moderate COVID-19 had shorter duration between onset symptoms and initial CT scan, which indicates that these patients could have presented at a relatively early stage of the disease. This was confirmed by the lower whole-lung and per-lobe QCT-PLO at baseline CT. Pulse oxygen saturation of all severe and critical type patients was less than 90%, and more than half had dyspnea, which concords to the higher lung opacification percentage assessed using the deep learning tool. According to prior studies (12,13), severe and critical type patients had multiple ground-glass opacities with consolidation, which can lead to ventilatory dysfunction and even respiratory failure. Moreover, hs-CRP was significantly elevated in severe and critical type patients, which indicates an inflammatory type of response.

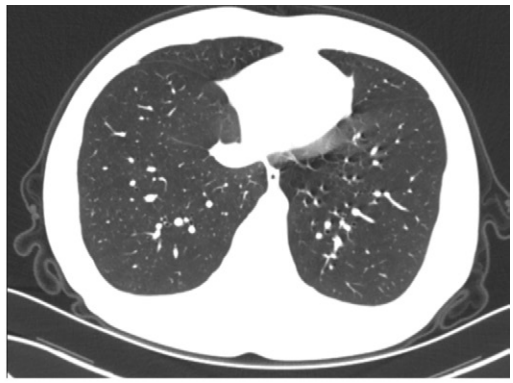

a.

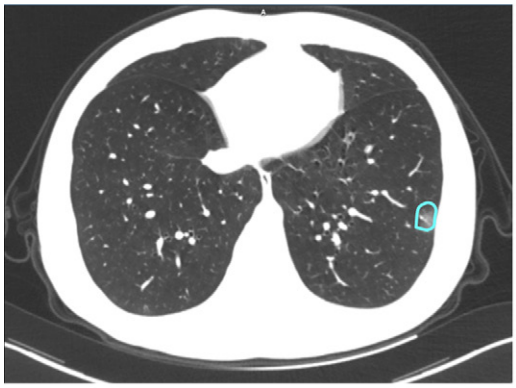

b.

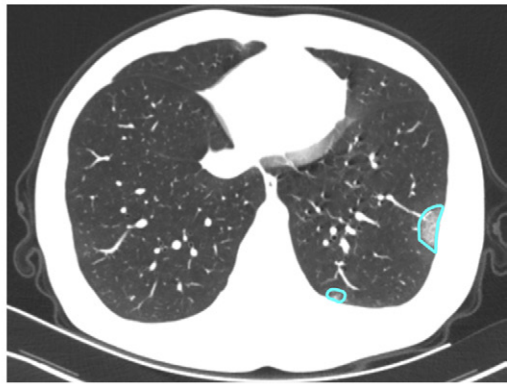

c.

Figure 3: A 29-year-old male patient with mild COVID-19, axial chest CT images at baseline and follow-up. **(a)** Baseline: negative CT; **(b)** first follow-up: ground-glass opacity is observed in the left lower lobe (opacification percentage of the left lower lobe: 0.24%); **(c)** second follow-up: increased size and new ground-glass opacity (opacification percentage of the left lower lobe: 2.55%).

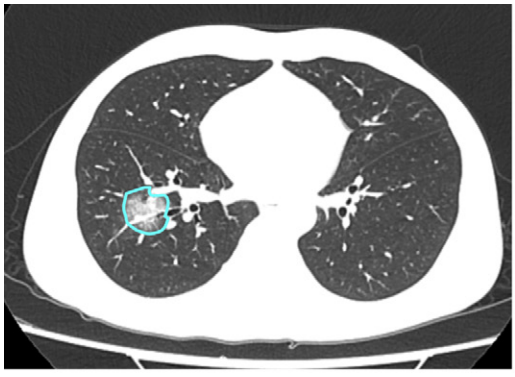

a.

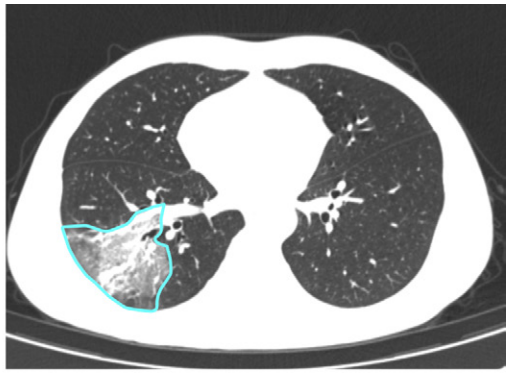

b.

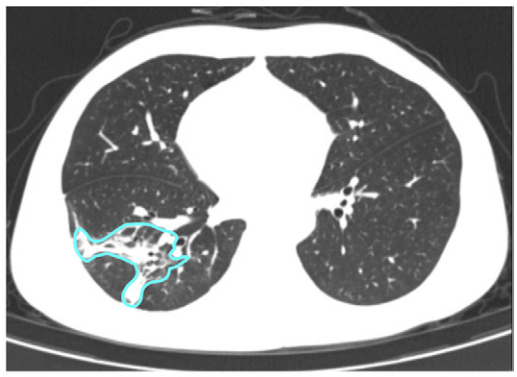

c.

Figure 4: A 41-year-old man with moderate COVID-19, axial chest CT images at baseline and follow-up. **(a)** Baseline: ground-glass opacity is found in the right lower lobe (opacification percentage of the right lower lobe: 1.33%); **(b)** first follow-up: increased patchy ground-glass opacity with new consolidation in the right lower lobe (opacification percentage of the right lower lobe: 12.56%); **(c)** second follow-up: ground-glass opacity is partially absorbed and development of perilobular pattern (opacification percentage of the right lower lobe: 9.28%).

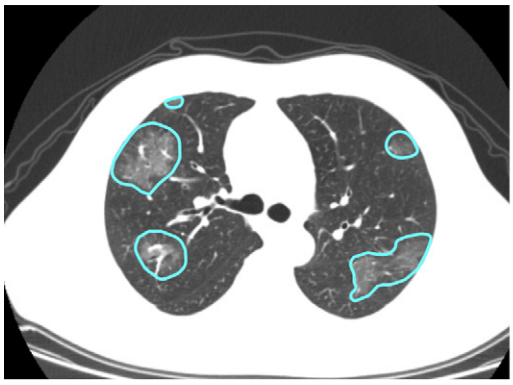

Figure 5: A 56-year-old man with severe COVID-19, axial chest CT images at baseline and follow-up. **(a)** Baseline: multiple ground-glass opacities are observed in the right and left upper lobes (opacification percentages of right and left lobes: 19.78% and 17.79%, respectively); **(b)** first follow-up: multiple patchy ground-glass opacities are increased bilaterally (opacification percentages of right and left lobes: 30.39% and 29.72%, respectively); **(c)** second follow-up: ground-glass opacity is absorbed, with development of consolidation and perilobular pattern (opacification percentages of right and left lobes: 24.21% and 19.73%, respectively).

a.

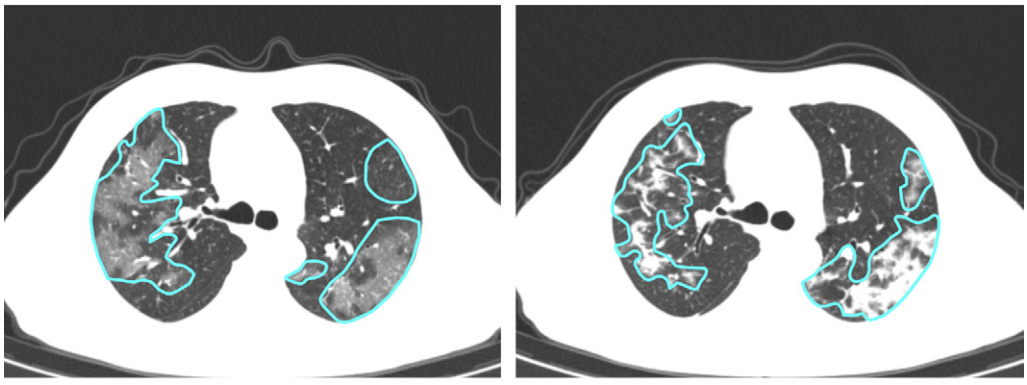

b. c.

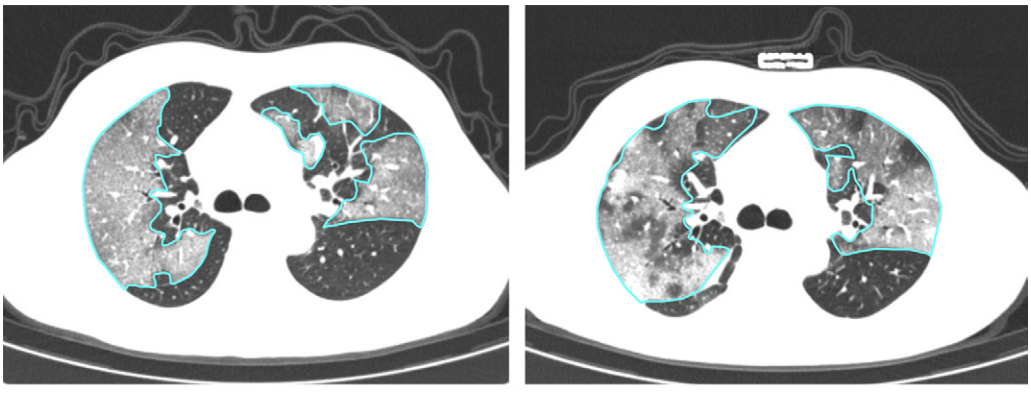

a. b.

Figure 6: A 53-year-old man with critical COVID-19, axial chest CT images at baseline and follow-up. **(a)** Baseline: multiple ground-glass opacities are observed in the right and left upper lobes (opacification percentages of right and left lobes: 53.55% and 45.89%, respectively); **(b)** first follow-up: multiple patchy ground-glass opacities are increased bilaterally, with development of consolidation (opacification percentages of right and left lobes: 59.36% and 67.77%, respectively).

We observed in our data that whole-lung and per-lobe QCT-PLO were higher at the first follow-up than at baseline, suggesting a sustained progression of imaging findings from presentation, plateauing on the second follow-up CT. Such pattern could be attributed to many factors, including the characteristics of our cohort, clinical severity at admission, treatment effect, and the natural history of disease. Depending on the initial clinical type and time of scan, patients could present at any of the stages described here. A combined analysis of our quantitative results suggests that pulmonary involvement in COVID-19 increases after the beginning of symptoms, peaking at 13 days, which is consistent with prior observation (9).

This study had several limitations. First, not all patients had a serial of three CT scans; therefore, we cannot systemically evaluate the changes for all patients at the first and second follow-up. Second, there was no systematic confirmation of the pulmonary opacities as being directly caused by the pathologic effects of the coronavirus. Finally, although the commercial software can quantitatively evaluate lung opacification percentage, the current version still needs radiologists' supervision. Noticeably, 13

of 148 (8.7%) of the cases did not have sufficient segmentation quality to ensure appropriate quantification.

In conclusion, the pulmonary involvement of COVID-19 could be objectively assessed by deep learning–based quantitative CT. This automated tool may be used for quantifying the disease burden and monitoring disease progression or response to treatment.

Disclosures of Conflicts of Interest: **L.H.** disclosed no relevant relationships. **R.H.** disclosed no relevant relationships. **T.A.** disclosed no relevant relationships. **P.Y.** disclosed no relevant relationships. **H.K.** disclosed no relevant relationships. **Q.T.** disclosed no relevant relationships. **L.X.** disclosed no relevant relationships.

Author contributions: Guarantor of integrity of entire study, L.X.; study concepts/study design or data acquisition or data analysis/interpretation, all authors; manuscript drafting or manuscript revision for important intellectual content, all authors; approval of final version of submitted manuscript, all authors; agrees to ensure any questions related to the work are appropriately resolved, all authors; literature research, L.H., R.H., T.A., L.X.; clinical studies, L.H., R.H., L.X.; experimental studies, L.H., P.Y., H.K.; statistical analysis, L.H.; and manuscript editing, L.H., P.Y., H.K., Q.T., L.X.

References

1. Huang C, Wang Y, Li X, et al. Clinical features of patients infected with 2019 novel coronavirus in Wuhan, China. Lancet 2020;395(10223):497–506 [Published correction appears in Lancet 2020;395(10223):496.].
2. Naming the 2019 Coronavirus. The International Committee on Taxonomy of Viruses (ICTV) website. https://talk.ictvonline.org. Published February 11, 2020. Accessed February 2020.
3. Up to March 16, the latest situation of new coronavirus pneumonia. National Health Commission of the People's Republic of China website. http://www.nhc.gov.cn/xcs/yqtb/202003/28d026a0422844969226913ee3d56d77.shtml. Published March 17, 2020. Accessed March 2020.
4. WHO Director-General's opening remarks at the media briefing on COVID-19-March 16, 20200. World Health Organization website. https://www.who.int/dg/speeches/detail/who-director-general-s-opening-remarks-at-the-media-briefing-on-covid-19---16-march-2020. Published March 16, 2020. Accessed March 2020.
5. Interim guidance: Clinical management of severe acute respiratory infection when novel coronavirus (nCoV) infection is suspected. World Health Organization website. https://www.who.int/publications-detail/clinical-management-of-severe-acute-respiratory-infection-when-novel-coronavirus-(ncov)-infection-is-suspected. Published January 28, 2020. Accessed February 2020.
6. Diagnosis and Treatment Protocol of Novel Coronavirus (trial version 5th). National Health Commission of the People's Republic of China website. http://www.nhc.gov.cn/yzygj/s7653p/202002/3b09b894ac9b4204a79db5b8912d4440.shtml. Published February 4, 2020. Accessed February 2020.
7. Xu Z, Shi L, Wang Y, et al. Pathological findings of COVID-19 associated with acute respiratory distress syndrome. Lancet Respir Med 2020 Feb 18 [Epub ahead of print]https://doi.org/10.1016/S2213-2600(20)30076-x.
8. MacMahon H, Naidich DP, Goo JM, et al. Guidelines for management of incidental pulmonary nodules detected on CT images: From the Fleischner Society 2017. Radiology 2017;284(1):228–243.
9. Pan F, Ye T, Sun P, et al. Time Course of Lung Changes On Chest CT During Recovery From 2019 Novel Coronavirus (COVID-19) Pneumonia. Radiology 2020 Feb 13:200370 [Epub ahead of print].
10. Science and technology anti-epidemic: inferVISION company first launched pneumonia AI system into clinical use. cn-healthcare website. https://www.cn-healthcare.com/article/20200131/wap-content-529622.html. Published January 31, 2020. Accessed February 2020.
11. Ronneberger O, Fischer P, Brox T. U-Net: Convolutional Networks for Biomedical Image Segmentation. In: Navab N, Hornegger J, Wells W, Frangi A, eds. Medical Image Computing and Computer-Assisted Intervention – MICCAI 2015. MICCAI 2015. Lecture Notes in Computer Science, vol 9351. Cham, Switzerland: Springer, 2015; 234–241.
12. Huang L, Han R, Yu X, et al. A correlation study of CT and clinical features of different clinical types of 2019 novel coronavirus pneumonia. Zhonghua Fang She Xue Za Zhi 2020;54:E003.
13. Song F, Shi N, Shan F, et al. Emerging 2019 Novel Coronavirus (2019-nCoV) Pneumonia. Radiology 2020;295(1):210–217.